

NASA TECHNICAL  
MEMORANDUM



N13-24088

NASA TM X-2810

NASA TM X-2810

**CASE FILE  
COPY**

PERFORMANCE OF ELECTRICAL SUBSYSTEM  
OF 2- TO 15-KILOWATT  
BRAYTON POWER CONVERSION SYSTEM

by Richard R. Secunde and James E. Vrancik

Lewis Research Center  
Cleveland, Ohio 44135

NATIONAL AERONAUTICS AND SPACE ADMINISTRATION • WASHINGTON, D. C. • JUNE 1973

|  |   |  |                             |
|--|---|--|-----------------------------|
| 1. Report No.<br><b>NASA TM X-2810</b>   | 2. Government Accession No.                                 | 3. Recipient's Catalog No.   |                             |
| 4. Title and Subtitle<br><b>PERFORMANCE OF ELECTRICAL SUBSYSTEM OF 2- TO 15-KILOWATT BRAYTON POWER CONVERSION SYSTEM</b>   |   | 5. Report Date<br>June 1973  |                             |
|  |   | 6. Performing Organization Code  |                             |
| 7. Author(s)<br>Richard R. Secunde and James E. Vrancik  |   | 8. Performing Organization Report No.<br><b>E-7366</b>   |                             |
|  |   | 9. Performing Organization Name and Address<br>Lewis Research Center<br>National Aeronautics and Space Administration<br>Cleveland, Ohio 44135 |                             |
|  |   | 10. Work Unit No.<br><b>503-35</b>   |                             |
| 12. Sponsoring Agency Name and Address<br>National Aeronautics and Space Administration<br>Washington, D. C. 20546   |   | 11. Contract or Grant No.  |                             |
|  |   | 13. Type of Report and Period Covered<br><b>Technical Memorandum</b>   |                             |
| 15. Supplementary Notes  |   | 14. Sponsoring Agency Code   |                             |
| 16. Abstract<br>The electrical subsystem of the 2- to 15-kilowatt Brayton power conversion system was evaluated under various operating and off-design temperature conditions in a vacuum environment. Overall operation was satisfactory. Speed controller operation is a major cause of distortion in the system ac voltage and current waveforms. This distortion has a small, but potentially significant effect on the performance of individual subsystem components.<br><i>Richard R. Secunde, James E. Vrancik</i> |   |  |                             |
| 17. Key Words (Suggested by Author(s))<br>Electrical Performance<br>Subsystem Power<br>Brayton   |   | 18. Distribution Statement<br><b>Unclassified - unlimited</b>  |                             |
| 19. Security Classif. (of this report)<br><b>Unclassified</b>  | 20. Security Classif. (of this page)<br><b>Unclassified</b> | 21. No. of Pages<br><b>24</b>  | 22. Price*<br><b>\$3.00</b> |

\* For sale by the National Technical Information Service, Springfield, Virginia 22151

PERFORMANCE OF ELECTRICAL SUBSYSTEM OF 2- TO 15-KILOWATT  
RAYTON POWER CONVERSION SYSTEM  
by Richard R. Secunde and James E. Vrancik  
Lewis Research Center

SUMMARY

The electrical subsystem of the 2- to 15-kilowatt Brayton power conversion system consists of the auxiliary electrical equipment required for an integrated, self-contained power conversion system. All of the electrical components with the exception of valve operators and gas storage bottle heaters are included. These components are the alternator, speed controller, alternator voltage regulator, dc power supply, batteries, two 400-hertz motor-driven pumps, two inverters to provide power for the pumps, an inverter for motor-starting the power conversion system, and the Brayton Engine Control System.

The electrical subsystem, with the Brayton alternator simulated by a motor-driven alternator, was evaluated under various system operating and off-design temperature conditions, including cold startup, in a vacuum environment in order to determine overall performance.

Overall operation of the electrical subsystem was satisfactory. Speed controller operation is a major cause of distortion in the system ac voltage and current waveforms. This distortion has a small, but potentially significant effect on the performance of individual subsystem components. The silver-cadmium batteries originally selected for use in the Brayton power conversion system failed after several cycles.

The subsystem performance was also evaluated during and after startup following a cold soak at temperatures as low as -50° C. These conditions had no significant effect on subsystem performance. Only minor inaccuracies in the temperature indicators and small changes in component efficiencies were observed.

INTRODUCTION

The NASA Lewis Research Center is investigating Brayton cycle electric power

generating systems capable of operation in a space environment. As described in reference 1, this development has resulted in the design and construction of a complete power system capable of producing from 2 to 15 kilowatts of electric power at 1200 hertz.

As part of the overall Brayton-cycle system, the electrical subsystem provides the required regulation and control of the generated electric power as well as control of the overall system. It provides electric power for auxiliary system components such as the coolant pumps. The speed of the turbine-driven alternator and, thereby, the frequency of the generated ac power is maintained by a parasitic-loading speed controller which utilizes phase-controlled loading. The term "phase control" as used in this report describes the action whereby the current through a device such as a controlled rectifier can be started at any selected time (electrical angle) during a half cycle of the applied voltage. The phase-controlled devices are used back-to-back electrically and full-wave control is available. References 2 and 3 describe the electrical subsystem and its performance as determined from previous tests.

This report includes some of the previous test results, describes recent improvements in the electrical subsystem, and presents the results of a program in which subsystem overall performance was experimentally evaluated. The evaluation included operation of the subsystem at various power levels within the 2- to 15-kilowatt range, cold startup followed by low-temperature operation, and operation with coolant temperatures above normal values. It was expected that phase control in the power stages of the parasitic-loading speed controller would have significant effects on the system voltages and currents. The operation of a transformer-rectifier dc supply in a small ac system causes a small, but noticeable, distortion in the system ac voltage. And, as reported in references 2 and 3, a significant ripple component exists on the dc bus voltage. Therefore, particular emphasis was placed on the effects of subsystem operation on user load power quality, component performance in the subsystem, and on intercomponent compatibility (i.e., how the performance of one component is affected by the simultaneous operation of other subsystem components).

These results presented in this report, although obtained from the testing of a particular set of components, are indicative of the performance which might be expected of similar systems.

## DESCRIPTION OF ELECTRICAL SUBSYSTEM

The Brayton electrical subsystem is designed for space operation and consists of the alternator, the electrical control package (ECP), the parasitic load resistors (PLR), the dc power supply, two batteries, two pump inverters, the Brayton control system (BCS), and an inverter to provide power for operation of the alternator as a motor for system startup.

For this evaluation, the two 400-hertz motor-driven coolant pumps, also referred to as pump-motor assemblies (PMA's), together with the cold plates and other coolant loop items required for the removal of heat from electrical subsystem components are considered parts of the electrical subsystem. Figure 1 shows a block diagram of this subsystem.

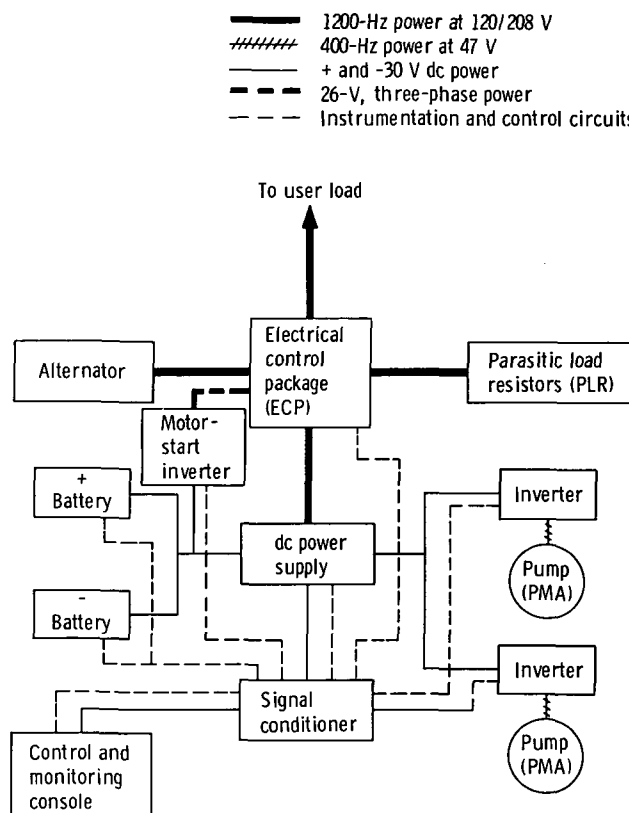


Figure 1. - Block diagram of Brayton electrical subsystem.

## Alternator

The alternator is a part of the Brayton Rotating Unit (BRU) assembly which also contains the turbine and compressor, all on a common shaft. This alternator, described fully in reference 4, is a modified Lundell, solid rotor machine. It is of four-pole construction and operates at 36 000 rpm to generate three-phase, 1200-hertz power at 120/208 volts. Cooling is by conduction to liquid coolant in dual passages around the alternator housing.

## Electrical Control Package

The ECP contains the speed controller, the alternator voltage regulator, user-load contactor, current transformers for measurement of alternator and load currents, and several additional circuits and contactors used for system control.

The PLR dissipates the excess power developed by the turbine-driven alternator. These resistors are located external to the ECP. The amount of power diverted to the PLR is controlled by the speed controller in the ECP so that the total load on the alternator is maintained relatively constant regardless of user (vehicle) load. This results in constant BRU speed. References 3 and 5 describe the ECP in more detail.

In order to permit small overloads without causing a system shutdown, a volts-per-hertz reference circuit has been incorporated into the alternator-voltage regulator to replace the fixed-voltage reference. Above the rated frequency, the alternator voltage remains relatively constant. Upon a small overload, it decreases linearly with decreasing frequency until a new power balance is achieved. Reference 6 describes the volts-per-hertz reference circuit in more detail.

A gas bottle heater control has also been incorporated into the ECP. It maintains the temperature of the Brayton system gas storage bottle at a predetermined level by means of on-off control of heating elements. A bimetal thermostatic control provides backup. Power for the bottle heater is drawn from the system battery bus.

## Direct Current Power Supply

The dc power supply converts ac power from the alternator to + and -30 volts dc to supply the electrical subsystem components. It is a polyphase, unregulated, transformer-rectifier type device without output filters. Two 28-volt batteries are included in the subsystem to provide dc power for subsystem operation during Brayton system startup and shutdown, and for short term backup power in the event of transformer-rectifier or alternator malfunction.

A complete description of the dc power supply along with component test results is presented in references 7 and 8.

## Coolant System

This Brayton power system uses two coolant loops to provide redundancy for component cooling. The electrical subsystem components are mounted on four dual-path cold plates connected in series. Normally, one loop operates while the other serves as

a standby. Each loop is independent and complete with a separate motor-driven pump. Inverters which are described in reference 9 provide ac power for driving the induction motors of the PMA's. An experimental evaluation of the pump is reported in reference 10 and of the inverters in reference 11.

### Motor-Start Inverter

A recent addition to the Brayton electrical subsystem is the motor-start inverter used to drive the alternator as a motor for system startup. This inverter, which is described in reference 12, converts dc power from the battery source to 400-hertz, three-phase power. By elimination of the originally used gas-injection starting procedure, motor starting the Brayton system results in reduced gas loss, less gas inventory, simplification of the gas management system, and multiple start capability.

### Brayton Control System

The BCS, as described in reference 13, provides the necessary control and monitoring for overall Brayton power system operation. It consists of two major assemblies, a signal conditioner, and a control and monitoring console. The signal conditioner is designed for space environment and is located with the Brayton power system.

The BCS has been modified slightly from that described in reference 13 to provide compatibility with the motor-start system and to improve overall performance. Two of the more significant modifications are described in the next paragraphs.

In the original design of the BCS, the speed of the alternator was determined by measuring the frequency of the generated ac voltage. A change was required because the Brayton engine is now started by motoring the alternator rather than by the gas-injection scheme first used. Also, for proper control action by the BCS, a more reliable means of speed indication was needed. Under electrical fault conditions, speed indication by means of the frequency of the generated ac voltage does not provide the required reliability. While motoring, there would be no usable frequency to measure speed during startup. To eliminate these problems, magnetic speed transducers were installed on the compressor scroll to sense compressor wheel speed (and thereby, alternator speed and frequency). Three of these pickups were required to maintain the same triple redundancy provided by the three-phase frequency sensors of the original design. Tests have verified that there is sufficient output from these magnetic transducers to measure the speed of the BRU to near-zero.

The second significant modification to the BCS was the improvement of the dc power supplies in the signal conditioner. The output of the original supplies had excessive noise and ripple which interferred with the proper operation of the conditioner circuits. Newly designed supplies which incorporate a NASA developed analog-signal-to-discrete-time-interval converter (ASDTIC) have been included in the present signal conditioner configuration. A detailed description of these supplies is contained in reference 14. The output of the new supplies contains less than 100 millivolts ripple and the regulation is better than the required  $\pm 1$  percent.

## EXPERIMENTAL APPROACH

### Brayton and Support Equipment

The Brayton electrical subsystem, less the alternator and the control and monitoring console was assembled on a frame as shown in figure 2. This simulates the actual Brayton system assembly as described in references 1 and 2. For all evaluations discussed in this report, the Brayton alternator was simulated with a variable-frequency, motor-driven alternator. The leakage reactance of the motor-driven alternator is approximately the same as that of the Brayton alternator. This simulation allows a high

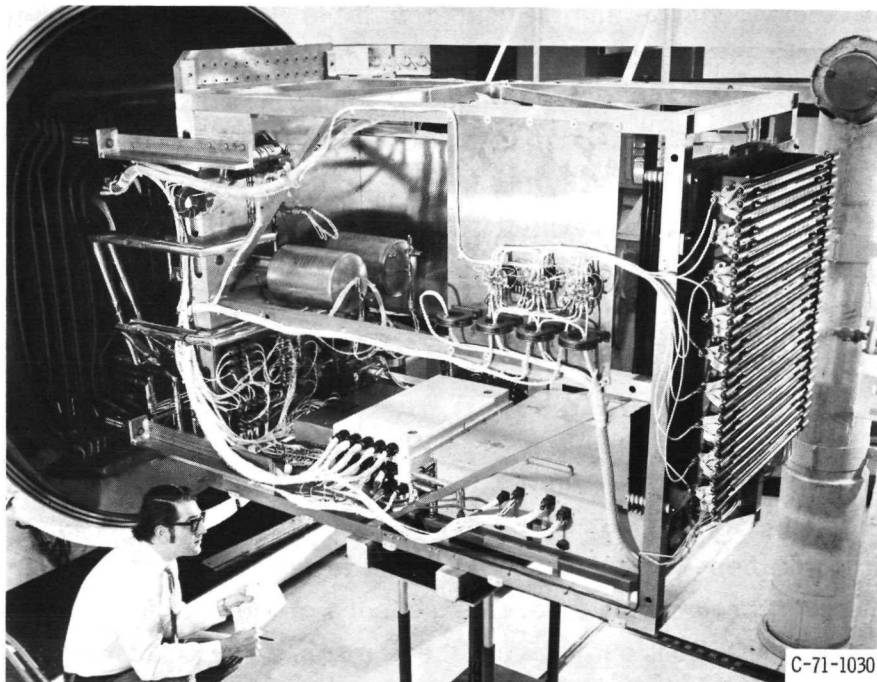


Figure 2. - Electrical subsystem evaluation assembly.

degree of flexibility in test conditions. The subsystem as shown in figure 2 is operable both inside a 1.8-meter- (6-ft-) diameter vacuum tank as well as in a room environment. The control and monitoring console of the BCS and the variable-frequency alternator are located external to the tank. Also, for flexibility, power to individual Brayton components can be disconnected by remotely controlled latching relays. Auxiliary power sources and loads are available to allow most components to be operated independently.

In order to be completely functional, the Brayton control system requires input signals from temperature, flow, pressure, and other transducers located on Brayton components which are not a part of the electrical subsystem. Such inputs come from the gas loop, turbine, compressor, and so forth. All the control functions which are operated by the BCS are within the electrical subsystem with the exception of electrically operated valves. The inputs to the BCS which are not available from the electrical subsystem are simulated with electrical signals. The electrically operated valves are simulated with relays. This simulation equipment is located external to the vacuum tank. The Brayton alternator fields (series and shunt) are simulated with a dual-winding inductor which provides loads for the alternator excitation circuits in the ECP.

All power, load, control, simulation, and instrumentation leads are brought through the vacuum tank bulkhead in connector-type feedthroughs.

The electrical subsystem and facility described previously is also used for endurance demonstration of Brayton components.

## Data Acquisition

The bulk of performance data was taken and partially reduced by a computer-controlled automatic data acquisition system. This system is similar to that described in reference 15, but without the disk memory. Also, in addition to the dc digital voltmeter, a true rms digital voltmeter was used. Power was measured with a special high-frequency wattmeter. The wattmeter was developed at Lewis Research Center and is described fully in reference 16.

In addition to the data collected by the data acquisition system, waveform data was obtained with a wave analyzer and a distortion meter. The automatic data system also measures frequency but uses a frequency-to-dc converter to do so. The expected 0.5 percent accuracy in the frequency-to-dc conversion produces a 6-hertz error in the 1200-hertz range. This amount of error is not tolerable when describing some aspects of electrical subsystem performance, such as speed controller operation. Therefore, a digital counter was used to accurately measure the alternator frequency.

## Test Procedure

In order to determine the effects of voltage distortion, harmonic currents, ripple voltages, and so forth, on overall performance, the electrical subsystem was operated under various combinations of alternator gross power, and parasitic load power.

Alternator gross power levels were 5, 10, and 15 kilowatts. It was assumed that the power factor (PF) of the user load would be 0.8, lagging. Various user loads were applied to the system with a resistive-reactive load bank. For each user-load setting, the system frequency was manually varied until the speed controller applied the amount of parasitic load necessary to bring the alternator gross power to the desired level. The measured parasitic load power included the loss in the power stages of the speed controller. The power to operate the electrical subsystem was included in alternator gross power. Under these conditions, data were taken and reduced to show the variations in losses, efficiency, distortion, neutral currents, and so forth.

The power drawn by the BCS from the dc bus under steady operating conditions varies in magnitude because of the cycling of the on-off controllers for the small thermocouple ovens which it contains. This cycling is approximately  $\pm 9$  percent of the BCS average power. The cycle time of these controllers was generally shorter than the  $3\frac{1}{2}$ -minutes scan time of the automatic data system. This scan time is the result of the 4-second reading time required for each true rms value. Therefore, to assure consistent results for the parts of this evaluation where overall subsystem losses were determined, the BCS load on the dc bus was simulated with a constant load equal to the BCS average.

To simulate a space environment, the electrical subsystem was operated in the vacuum tank at an ambient pressure of less than  $1.33 \times 10^{-3}$  newton per meter squared ( $1 \times 10^{-5}$  torr). For all of the tests discussed in this report, except those concerned with cold start and off-design temperature performance, the temperature of the coolant into the cold plates was maintained at the design value of  $+20^{\circ}\text{C}$ . Test conditions or procedures which were used for the various particular phases of this evaluation are described in the section DISCUSSION OF RESULTS.

Subsystem component temperatures as well as the temperature of critical parts within the components were monitored during all test conditions. Where large changes in temperature were observed, the test condition was maintained and data were taken after those temperatures were within 10 percent of their final value.

## DISCUSSION OF RESULTS

When an alternator is supplying a linear load, the load voltage waveform is gener-

ally sinusoidal. However, with the same total load, the distortion in this voltage will increase when nonlinear elements such as thyristors or common rectifiers are part of that load. The degree of distortion will depend primarily on the nature and magnitude of the nonlinear load and the alternator leakage reactance. The speed controller with its controlled rectifiers is a variable nonlinear load. In the Brayton alternator the leakage reactance is in the order of 0.8 ohm. The motor-driven alternator used to simulate the Brayton alternator has a similar leakage reactance value in the order of 0.9 ohm. These values were verified experimentally from the phase conduction overlap existing when a polyphase rectified load was connected to the alternators. Therefore, the effects on alternator and load voltage as determined with the motor-driven alternator approximate those which exist with the Brayton alternator.

In order to provide a reference so that the effects of electrical subsystem operation can be better appreciated, the user-load voltage waveform with the Brayton dc power supply disconnected and the speed controller operation inhibited off (no parasitic load) is shown in figure 3. This voltage waveform was obtained with the user load set at 10 kilowatts, 0.8 PF lagging. The total harmonic distortion is approximately 2 percent with a predominant fifth harmonic.

Capacitors are used in the ECP to filter high-frequency electrical noise on the 1200 hertz power lines generated by the speed controller during normal operation. These capacitors are connected to the ac voltage lines and present a leading power factor load of approximately 2 KVAR (kilovolt-ampere reactive) to the alternator. As a result of this leading power factor load and the 0.8 PF lagging user load the net alternator power factor was 0.9, lagging, in the reference test.

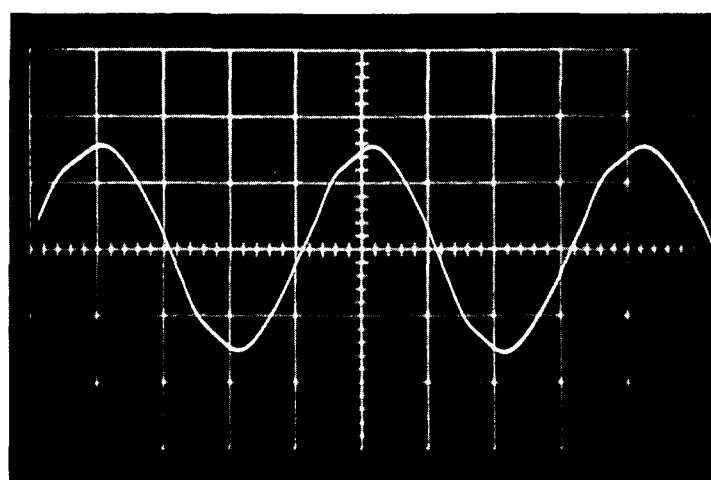


Figure 3. - User-load voltage wave shape without dc supply or parasitic loads. User load, 10 kilowatts; power factor, 0.8; distortion, 2 percent; predominant harmonic, fifth.

## Direct Current Power Supply Performance

The Brayton dc power supply provides approximately 800 watts for steady-state subsystem operation. This does not include the intermittent power required for battery charging and gas bottle heating.

Transformer-rectifier circuits in the dc power supply convert 1200 hertz ac power from the alternator to + and -30 volts dc. The effect of dc supply operation on the user-load wave shape is shown in figure 4. This wave shape exists with steady-state subsys-

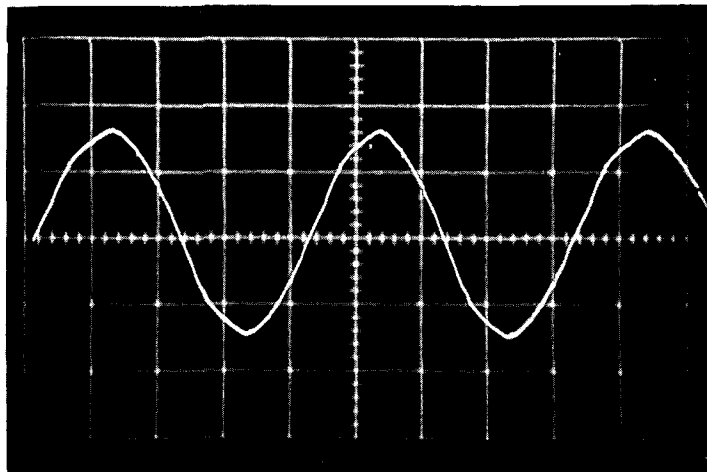


Figure 4. - User voltage wave shape as effected by normal dc supply operation in subsystem. Alternator gross output power, 10 kilowatts; user load, 9 kilowatts; power factor, 0.8; distortion, 2 percent; predominant harmonics, third and fifth.

tem operation and speed controller operation inhibited off. The effect is very small, being the slight notching in the waveform. There is also an increase in the third harmonic component and a reduction in the fifth. The total harmonic distortion remained at approximately 2 percent with approximately equal magnitudes of the third and fifth harmonics. The notching is the result of rectifier commutation, and the presence of the third harmonic is a result of the nonlinear input impedance of the transformers.

In normal system operation, the load on the dc supply is not balanced between the positive and negative 30-volt lines. The inverters are a balanced load, but the BCS power is approximately 0.22 kilowatt from the positive line and 0.04 kilowatt from the negative line. The total power load on the dc supply is approximately 0.5 kilowatt on the positive line and 0.3 kilowatt on the negative line.

The operation of the dc supply causes a neutral current in the 1200 hertz ac system of between 2 and 4 amperes. A typical waveform of this current is shown in figure 5.

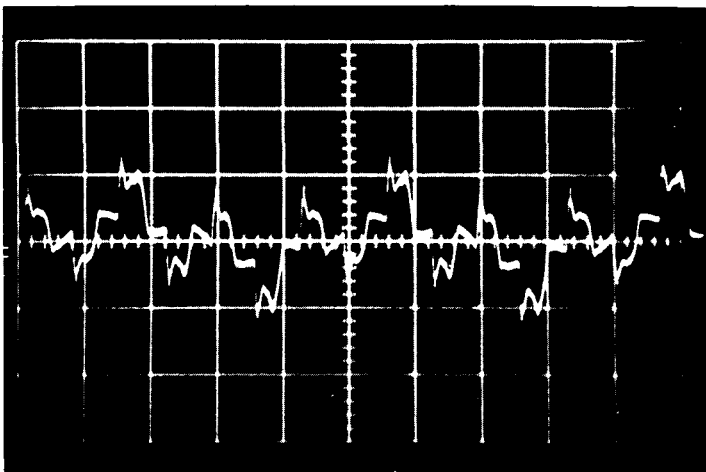


Figure 5. - Direct current supply neutral current waveform. Predominant frequency, 3600 hertz; total harmonic content, 178 percent of 1200-hertz component; rms value, 2.0 amperes.

The predominant frequency is third harmonic, the magnitude of which is approximately 160 percent of the fundamental (the fundamental being 1200 Hz). The total harmonic content is 178 percent of the fundamental.

With the speed controller inhibited off, the efficiency of the dc supply when providing dc power for all subsystem steady-state functions is approximately 88 percent. The dc output voltage is unfiltered and contains a ripple component which varies in magnitude depending on the amount of distortion in the system ac voltage. The minimum ripple on the 30 volt lines observed in this evaluation was approximately 6 volts peak-to-peak. This minimum occurred with the speed controller operation inhibited. The predominant ripple frequency is 14.4 kilohertz as would be expected with the rectifier circuit used. Reference 8 presents additional test data for the Brayton dc power supply.

The batteries originally used in the subsystem were of a sealed, silver-cadmium type with an 85 ampere-hour rating. The capacity of these batteries dropped below 85 ampere-hours after several charge-discharge cycles. Within 1 or 2 cycles after the noted capacity reduction, cell failures caused by silver penetration through the separators occurred. The failures occurred approximately 1.5 to 2 years after manufacture of the cells. Prior to operation in the subsystem, the batteries had been stored at room temperature in an undetermined state of charge. The subsystem was subsequently operated with simulated batteries in the absence of system batteries.

## Pump Inverter Performance

The pump inverter provides approximately 415 watts of 400-hertz, three-phase ac

power for the operation of the coolant pump. The input power is obtained from the dc lines as a two-wire input, giving an inverter nominal input voltage of 60 volts.

The measured efficiency of the inverters when driving the coolant pumps at normal flow conditions of  $1.2 \times 10^{-2}$  cubic meter per minute (3.18 gal/min) with a pressure rise of 48 newtons per centimeter squared (70 psi) is approximately 78 percent. Reference 11 provides additional inverter performance data. The ripple on the dc bus in the fully functioning electrical subsystem is not transmitted through the inverter to the inverter ac output voltage and had no noticeable effect on normal inverter performance.

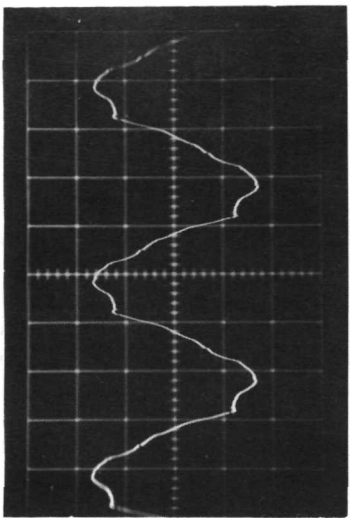
## Subsystem Component Interactions

As the speed controller changes parasitic load in response to varying frequency resulting from varying user loads, the effects of the phase control in the speed controller power stages will vary. The operation of the Brayton speed controller and its effects on the Brayton alternator armature current are described in reference 5. This section describes the effects of speed controller operation on the electrical subsystem and the net effects of speed controller and subsystem operation on user-load voltage.

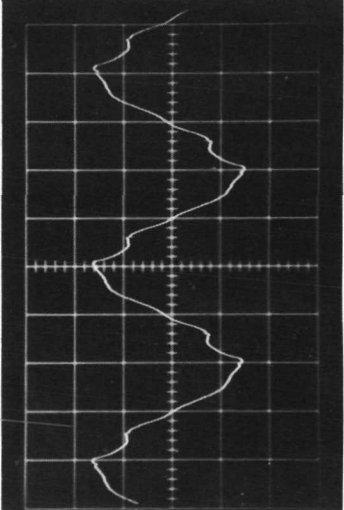
System and user-load ac voltage. - Photographs which show the effect of phase-controlled conduction in the parasitic load on the waveform of the user 1200-hertz voltage are shown in figure 6.

The wave shapes of figure 6(a) are representative of those obtained at the 5-kilowatt alternator gross power level. Those of figures 6(b) and (c) were obtained at the 10- and 15-kilowatt levels. The actual shape varies with parasitic load; therefore, the total distortion in user voltage wave shape, as measured with the distortion meter, is shown in figure 7 as a function of parasitic load power. Although the data for figure 7 was obtained with three different gross power levels, a general trend shown by the single plotted line is evident. The minimum distortion of approximately 3 percent occurs at minimum parasitic load. This is slightly higher than the distortion with only the dc supply because the minimum parasitic load varied between 0 and 100 watts and the power control circuitry of the speed controller was active. The maximum measured distortion of between 12 and 14 percent occurs with parasitic loads near 4 and 13 kilowatts. These distortions are the net effect of the parasitic load, user load, and electrical subsystem loads.

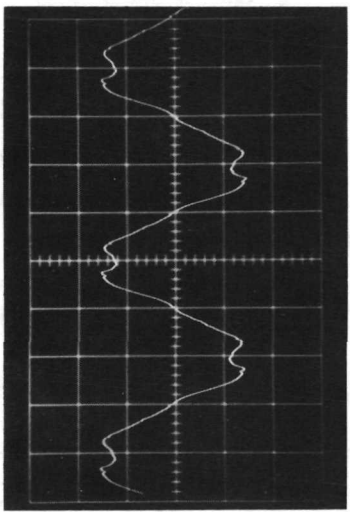
The data in figures 6 and 7 for the 10-kilowatt alternator gross power level are similar to those presented in reference 5. The data at the 5- and 15-kilowatt power levels provide additional information to describe the performance of the electrical subsystem over the range of power of which the Brayton power system is capable.



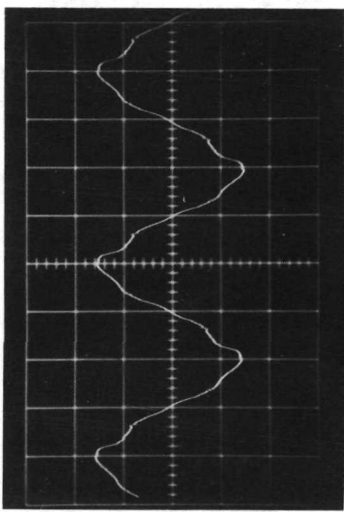
(a-1) 0.4-Kilowatt parasitic load (1204 Hz); distortion, 4.1 percent; predominant harmonics, fifth and seventh.



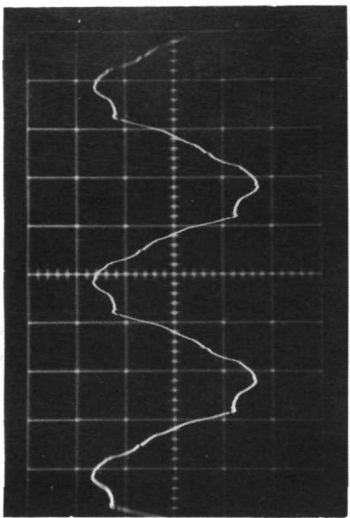
(a-2) 1.8-Kilowatt parasitic load (1214 Hz); distortion, 9.2 percent; predominant harmonics, third, fifth, and seventh.  
(a) Alternator gross output power, 5 kilowatts.



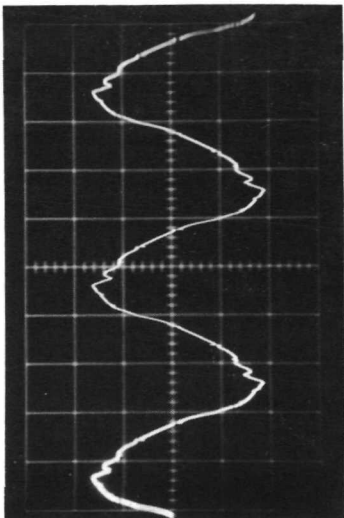
(b-1) 4.3-Kilowatt parasitic load (1222 Hz); distortion, 11.0 percent; predominant harmonics, third and fifth.



(b-2) 7.5-Kilowatt parasitic load (1230 Hz); distortion, 8.0 percent; predominant harmonics, third and fifth.  
(b) Alternator gross output power, 10 kilowatts.



(c-1) 6.3-Kilowatt parasitic load (1227 Hz); distortion, 9.0 percent; predominant harmonic, fifth.



(c-2) 11.3-Kilowatt parasitic load (1241 Hz); distortion, 11.0 percent; predominant harmonic, third.  
(c) Alternator gross output power, 15 kilowatts.

Figure 6. - User voltage wave shapes.

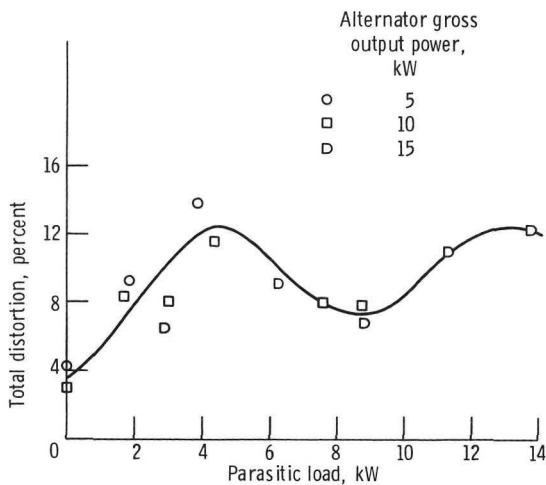


Figure 7. - User-load voltage total distortion as a function of parasitic load.

Unbalanced conduction in the speed controller power stages induces an unbalance in the rms three-phase system voltage. This unbalance is in addition to any unbalance present under conditions of no parasitic load. In the reference operation test (no parasitic load and no dc power supply) there was a 2.7-volt difference between the maximum and minimum user-load phase voltages. The change in unbalance is variable with operating conditions and not readily predictable. The maximum observed difference was 5.1 volts at a 1.3-kilowatt parasitic load with the alternator at the 15-kilowatt gross power level.

Direct current power. - The variation in distortion of the 1200-hertz ac voltage is transferred through the dc power supply to the dc lines as a variation in ripple. Figure 8 shows the variation in dc voltage ripple as a function of parasitic load. As in figure 7, the data shown in figure 8 were obtained with three different gross power levels. The single plotted line shows the general trend. The ripple generally is minimum at mini-

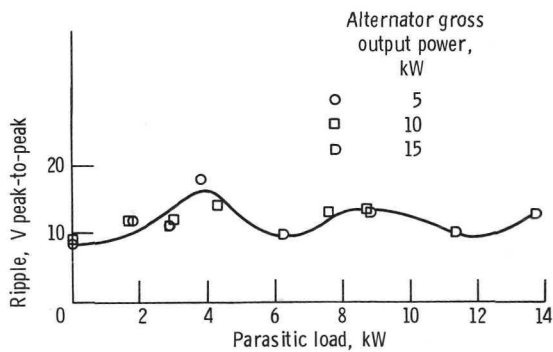


Figure 8. - Direct current power supply output voltage ripple as a function of parasitic load.

mum parasitic load. The minimum shown on this figure is approximately 2 volts higher than the minimum obtained with the speed control circuit inhibited off. This is a result of the nonzero minimum parasitic load mentioned previously which caused a slight distortion in the ac voltage. The maximum ripple observed was approximately 18 volts peak-to-peak on the +30-volt line. The parasitic load at which maximum ripple will occur is difficult to predict since the ripple is the net effect of the rectifier circuit used and the ac voltage wave shape. Unbalanced conduction in the parasitic load phases and induced transient spikes further complicate such a prediction.

Neutral current. - The phase control of the parasitic load causes a current to exist in the neutral of the alternator. The magnitude of this current and its variation with parasitic load are discussed in reference 5. The frequency of this current is approximately 3600 hertz or the third harmonic of the frequency of the alternator voltage. The maximum value of neutral current observed in this subsystem evaluation was 20 amperes with a nominal 10-kilowatt alternator gross power and a parasitic load of approximately 8.8 kilowatts. The user load was zero. This value of neutral current is the net result of neutral current from the dc supply and from the parasitic load. These two neutral currents are not in phase and have different harmonic components. At this load condition, the parasitic load neutral current was approximately 19 amperes and the dc supply neutral current was approximately 3 amperes.

Power factor. - The total electrical subsystem is a load of approximately 1.1 kilowatt if the alternator losses and parasitic load are not included. The dc power supply which is the major subsystem load has an input power factor of about 0.89 lagging when there is no parasitic load. Power factor as used in this report is the ratio of average real power (watts) to rms volt-amperes. As the parasitic load is increased by the speed controller, the power factor of the dc supply varies because of the changing harmonic content of the system ac voltage. The general trend of this variation in power factor is shown by the single line in figure 9. The lower power factor conditions could result in

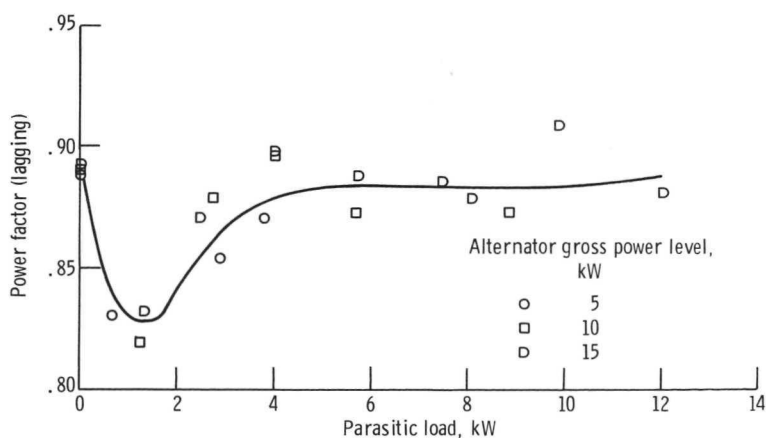


Figure 9. - Brayton dc power supply power factor as a function of parasitic load.

increased losses in the dc supply and associated temperature increases.

The power factor of the parasitic load varies as shown in figure 10. Phase control is similar in effect to a reactive component in the load. This is explained more fully in references 17 and 18. The power factor as seen by the alternator in this electrical subsystem is shown as a function of parasitic load in figure 11. The data in this figure were obtained with the user load PF at 0.8 lagging. As the figure shows, the power factor of the total load on the alternator is always nearer unity than the power factor of the user load. This is the result of the capacitors in the ECP and the higher power factor of the dc supply. These offset the low power factor of the parasitic load at low parasitic load values.

Subsystem losses. - The electrical subsystem power loss is defined as the result of a subtraction of user load power, alternator field power, and parasitic load power from the alternator output power. This power loss has also been called "housekeeping

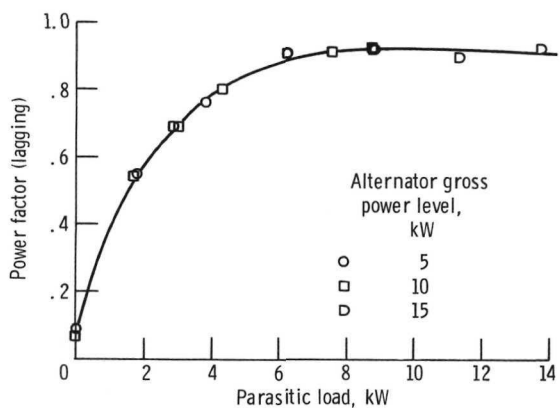


Figure 10. - Parasitic load power factor as a function of parasitic load.

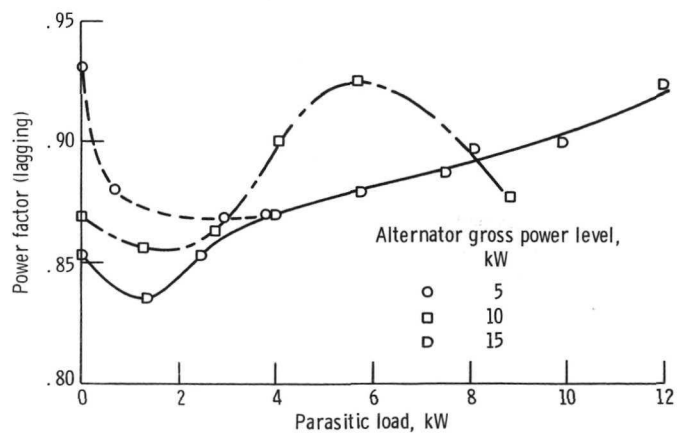


Figure 11. - Alternator power factor as a function of parasitic load.

power." The harmonic currents and voltages associated with the phase control in the parasitic load affect individual component losses in the subsystem. This fact is evidenced around the 4-kilowatt parasitic load condition by a significant increase in the temperature of the alternator field supply current transformers located in the ECP. The maximum distortion on the user-load voltage also occurs at this condition. The efficiency of the dc power supply varies between the 88 percent value obtained with zero parasitic load and a minimum value of 85.6 percent at 1.3-kilowatt parasitic load with the alternator gross power at the 15-kilowatt level.

The electrical subsystem loss, therefore, varies with parasitic load power. This variation is shown in figure 12 with the general trend shown by the single line. The

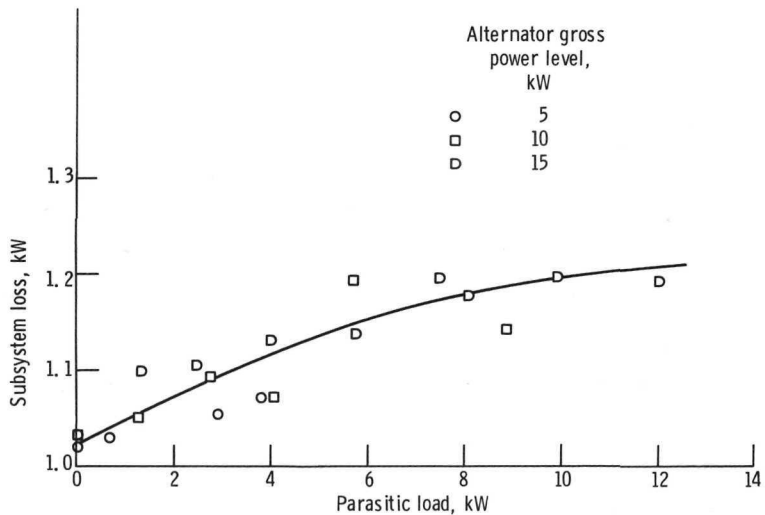


Figure 12. - Electrical subsystem loss as a function of parasitic load.

losses are generally higher at the 15-kilowatt system power levels because of the greater power required by the alternator fields and the increased losses in the power handling components in the ECP.

The power dissipated by the various subsystem components varies with system operating conditions as described in preceding sections of this report. Values of power lost under typical operating conditions at 5-, 10-, and 15-kilowatt alternator gross power levels are given in table I. The three conditions in table I are all with approximately the same parasitic load. Under this situation the changes in loss as power level varies are almost totally in the ECP.

TABLE I. - SUBSYSTEM COMPONENT LOSSES

|                          | Nominal alternator gross output power,<br>kW |           |           |
|--------------------------|--|-----------|-----------|
|                          | 5  | 10        | 15        |
| Parasitic load, kW       | 2.93   | 2.75      | 2.48      |
| Losses, kW:              |  |           |           |
| ECP                      | 0.12   | 0.18      | 0.19      |
| DC supply                | 0.12   | 0.12      | 0.12      |
| Inverter                 | 0.11   | 0.12      | 0.12      |
| BCS power                | 0.26±0.02                                    | 0.26±0.02 | 0.26±0.02 |
| Motor-driven pump power  | 0.43   | 0.41      | 0.42      |
| Total subsystem loss, kW | 1.04±0.02                                    | 1.09±0.02 | 1.11±0.02 |

## Performance Under Off-Design Temperature Conditions

Cold startup and low-temperature operation. - In a space environment, the Brayton system will be subjected to low-temperature extremes before and during startups. The performance of components and system interactions were investigated over an initial temperature range of 25° to -50° C. This was achieved by cold-soaking the nonoperating electrical subsystem to the specified temperatures prior to each simulated startup. The methods used for these investigations and the detail results are given in reference 19.

When the desired condition was reached, the subsystem was energized. All subsystem functions were available immediately, although temperature readings from the BCS were not stable and the heat source overtemperature control interlock in the BCS opened. When the thermocouple calibration ovens in the signal conditioner reached operating temperature (after ~30 min with the -50° C start temperature), the temperature readouts were correct. During the period immediately following (within 20 min) startup from cold soak conditions in the range of 25° to -50° C, small variations in the efficiency of some components were observed. Also some small changes in alarm set points occurred, probably the result of changes in amplifier characteristics in the BCS.

As shown in figure 13 the efficiency of the inverter-motor-pump combination decreased from 16 to 13 percent as the temperature decreased. The inverter efficiency went up due to a decrease in semiconductor losses and increased load. The efficiency of the motor-driven pump decreased due to the increase in viscosity of the coolant oil causing a 15-percent reduction in flow, and a 10-percent reduction in hydraulic power output.

The speed control characteristics and the output voltages of the inverter and dc supply were independent of temperature.

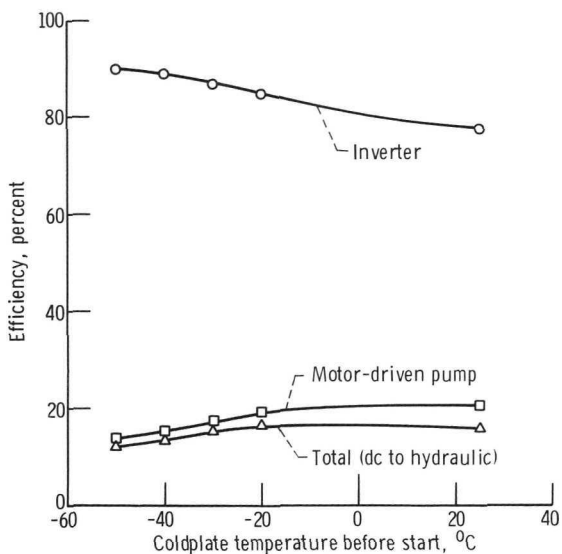


Figure 13. - Initial efficiency of secondary inverter and motor-driven pump after cold start.

Subsystem component performance during the cold start and low temperature tests is indicative of the performance which could be expected with low coolant temperature. These results gave no indication that there would be any problem starting the Brayton power conversion system from cold soak at low temperatures down to  $-50^{\circ}\text{C}$ .

Operation at elevated temperature. - In the event of abnormal cooling conditions, it is possible that the temperature of the coolant flowing into the cold plates will rise above the normal  $20^{\circ}\text{C}$ . To investigate performance trends as the coolant temperature increases, the coolant in the primary loop was circulated without rejection of the heat removed from the Brayton components to a sink. This caused the coolant temperature to rise slowly at a rate of about  $9^{\circ}\text{C}$  per hour or less. The secondary coolant loop was inactive.

With the alternator gross power level at 10 kilowatts, a user load of 6 kilowatts, 0.8 power factor lagging, and using the procedure described above, the average cold-plate coolant temperature was allowed to rise to approximately  $54^{\circ}\text{C}$ . During this period, no significant change in overall subsystem performance was observed. However, the efficiencies of the primary inverter and motor-driven pump, as shown in figure 14, continued the trends evidenced in the results of the low temperature tests which used the secondary coolant loop. The efficiency of the primary pump used in the elevated temperature test is generally higher than that of the secondary pump used in the cold start tests. As described in reference 10, this is probably due to the out-of-tolerance diffuser in the secondary pump. The hydraulic power output from the pump remained essentially constant at approximately 102 watts as temperature changed from  $27^{\circ}$  to  $54^{\circ}\text{C}$ . The increase in efficiency of the motor-driven pump is due most probably to the lower

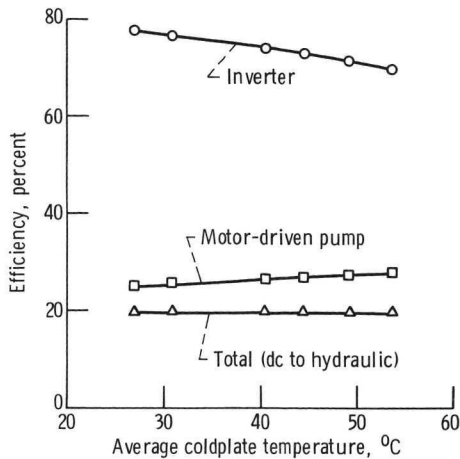


Figure 14. - Efficiency of primary inverter and motor-driven pump at elevated temperature.  
Pump hydraulic output power, ~100 watts.

oil viscosity and reduced drag in the flooded motor (see ref. 10). The power factor of the motor dropped from approximately 0.59 at  $27^{\circ}\text{C}$  to 0.55 at  $54^{\circ}\text{C}$ . The decrease in inverter efficiency shown in figure 14 is primarily a result of the reduced load imposed by the pump. As shown in reference 11, the efficiency of this inverter with the pump motor as a load is heavily dependent on the load magnitude. The net effect of the inverter and pump efficiency changes is an essentially constant efficiency of conversion from dc electric to hydraulic power over the temperature range of  $20^{\circ}$  to  $54^{\circ}\text{C}$ .

These results, although obtained at one particular alternator gross power level and user load, are indicative of the trends in performance change with temperature which can be expected at other power levels.

## CONCLUDING REMARKS

The operation of the phase-controlled, parasitic-loading speed controller induces a 3- to 14-percent distortion into the waveform of the voltage supplied by the electrical subsystem for user loads. The speed controller operation also has a small, but potentially significant, effect on the performance of other subsystem components. Subsystem losses, alternator power factor, neutral current, and dc bus voltage ripple vary with the amount of parasitic load. Interactions among subsystem components are small but should be considered in the design and application of an electrical power generating system of this type.

The recent improvements in the Brayton electrical subsystem include an inverter designed to motor start the power conversion system, magnetic speed transducers, new

power supplies for the control system, and a volts-per-hertz reference for the alternator voltage regulator.

The motor start technique allows reduced gas inventory, simplifies the gas management system, and allows a multiple startup capability. The magnetic speed pickups sense speed independently of the alternator output. This is essential for motor start operation. The new power supplies provide improved stability and efficiency for the control system, and the volts-per-hertz reference circuit gives the Brayton power conversion system greater tolerance to transient overloads.

Tests at low temperatures indicated that there would be no problem starting the Brayton power system from a cold soak temperature of -50° C. Operation of the subsystem with coolant temperatures from -50° to 50° C was satisfactory.

Lewis Research Center,  
National Aeronautics and Space Administration,  
Cleveland, Ohio, April 3, 1973,  
503-35.

## REFERENCES

1. Klann, John L.; and Wintucky, William T.: Status of the 2- to 15-kWe Brayton Power System and Potential Gains from Component Improvements. Intersociety Energy Conversion Engineering Conference. SAE, 1971, pp. 195-201.
2. Nestor, James; Thollot, Pierre A.; and Bainbridge, Richard C.: Electrical Subsystem for a 2- to 15-Kilowatt Brayton Power Conversion System. NASA TM X-2495, 1972.
3. Secunde, R. R.; Vrancik, J. E.; and Spagnuolo, A. C.: Experimental Evaluation of the Electrical Subsystem of the 2- to 15-kW Brayton Power Conversion System. Proceedings of the Intersociety Energy Conversion Engineering Conference. SAE, 1971, pp. 229-238.
4. Repas, David S.; and Edkin, Richard A.: Performance Characteristics of a 14.3-Kilovolt-Ampere Modified Lundell Alternator for a 1200 Hertz Brayton-Cycle Space-Power System. NASA TN D-5405, 1969.
5. Ingle, Bill D.; Wimmer, Heinz L.; and Bainbridge, Richard C.: Steady-State Characteristics of a Voltage Regulator and a Parasitic Speed Controller on a 14.3-Kilovolt-Ampere, 1200-Hertz Modified Lundell Alternator. NASA TN D-5924, 1970.

6. Wimmer, Heinz L.: Experimental Evaluation of a Volts-Per-Hertz Reference Circuit for the Isotope Brayton System. NASA TM X-2502, 1972.
7. Kruse, M.: DC Power Supply Engineered Magnetics Model EMPS-252 for Brayton Cycle Power Conversion System. Rep. FR-2390, Gulton Industries, Inc. (NASA CR-72529), Aug. 27, 1970.
8. Vrancik, James E.: Performance of a Direct-Current Power Supply for the 2- to 15-Kilowatt Brayton Cycle System. NASA TM X-2349, 1971.
9. Lachenmeier, G.: Design and Manufacture of Static Inverter for Brayton Power Conversion System. Rep. 2403, Gulton Industries, Inc. (NASA CR-72671), Dec. 3, 1969.
10. Spagnuolo, Adolph C.; Secunde, Richard R.; and Vrancik, James E.: Performance of a Hermetic Induction Motor-Driven Pump for Brayton Cycle Heat Rejection Loop. NASA TM X-52698, 1969.
11. Birchenough, Arthur G.; and Secunde, Richard R.: Performance Evaluation of Brayton Space Power System 400-Hertz Inverters. NASA TM X-2141, 1970.
12. Frye, Robert J.; and Birchenough, Arthur G.: Design of a Three-Phase, 15-Kilovolt-Ampere Static Inverter for Motor-Starting a Brayton Space Power System. NASA TN D-6602, 1971.
13. Thomas, Ronald L.; Bilski, Raymond S.; and Wolf, Robert A.: Requirements, Design, and Performance of a Control System for a Brayton Cycle Space Power System. Presented at the AIAA 5th Intersociety Energy Conversion Engineering Conference, Las Vegas, Nev., Sept. 21-25, 1970.
14. Vrancik, James E.; and Bainbridge, Richard C.: Improvements in and Test Results for the 2- to 15-kWe Brayton Cycle Electrical Subsystem. NASA TM X-2757, 1973.
15. Edkin, R. A.; Macosko, R. P.; and Kruchowy, R.: Automated Endurance Testing of a Brayton Power Conversion System. Proceedings of the Intersociety Energy Conversion Engineering Conference. SAE, 1971, pp. 202-210.
16. Vrancik, James E.: Design and Performance of a High-Frequency Wattage-to-Voltage Converter. NASA TN D-5674, 1970.
17. Gilbert, Leonard J.: Reduction of Apparent-Power Requirement of Phase-Controlled Parasitically Loaded Turboalternator by Multiple Parasitic Loads. NASA TN D-4302, 1968.

18. Perz, Dennis A.; and Valgora, Martin E.: Experimental Evaluation of Volt-Ampere Loading and Output Distortion for a Turboalternator with Multiple Load Phase-Controlled Parasitic Speed Controller. NASA TN D-5603, 1969.
19. Vrancik, James E.; and Bainbridge, Richard C.: Cold Startup and Low Temperature Performance of the Brayton Cycle Electrical Subsystem. NASA TM X-67995; 1971.

and the vibration system

**Page Intentionally Left Blank**

NATIONAL AERONAUTICS AND SPACE ADMINISTRATION  
WASHINGTON, D.C. 20546

OFFICIAL BUSINESS  
PENALTY FOR PRIVATE USE \$300

SPECIAL FOURTH-CLASS RATE  
BOOK

POSTAGE AND FEES PAID  
NATIONAL AERONAUTICS AND  
SPACE ADMINISTRATION  
451



POSTMASTER : If Undeliverable (Section 158  
Postal Manual) Do Not Return

*"The aeronautical and space activities of the United States shall be conducted so as to contribute . . . to the expansion of human knowledge of phenomena in the atmosphere and space. The Administration shall provide for the widest practicable and appropriate dissemination of information concerning its activities and the results thereof."*

—NATIONAL AERONAUTICS AND SPACE ACT OF 1958

## NASA SCIENTIFIC AND TECHNICAL PUBLICATIONS

**TECHNICAL REPORTS:** Scientific and technical information considered important, complete, and a lasting contribution to existing knowledge.

**TECHNICAL NOTES:** Information less broad in scope but nevertheless of importance as a contribution to existing knowledge.

**TECHNICAL MEMORANDUMS:** Information receiving limited distribution because of preliminary data, security classification, or other reasons. Also includes conference proceedings with either limited or unlimited distribution.

**CONTRACTOR REPORTS:** Scientific and technical information generated under a NASA contract or grant and considered an important contribution to existing knowledge.

**TECHNICAL TRANSLATIONS:** Information published in a foreign language considered to merit NASA distribution in English.

**SPECIAL PUBLICATIONS:** Information derived from or of value to NASA activities. Publications include final reports of major projects, monographs, data compilations, handbooks, sourcebooks, and special bibliographies.

**TECHNOLOGY UTILIZATION PUBLICATIONS:** Information on technology used by NASA that may be of particular interest in commercial and other non-aerospace applications. Publications include Tech Briefs, Technology Utilization Reports and Technology Surveys.

*Details on the availability of these publications may be obtained from:*

### SCIENTIFIC AND TECHNICAL INFORMATION OFFICE

NATIONAL AERONAUTICS AND SPACE ADMINISTRATION

Washington, D.C. 20546